DOI: 10.1002/ ((please add manuscript number))
Article type: Full Paper

Title: Electron-beam induced water removal, phase change and crystallization of anodic-electrodeposited turbostratic nickel hydroxide-oxyhydroxide

Kin Wa Kwan, Degang Xie, Rongrong. Zhang Zhiwei. Shan, Alfonso H. W. Ngan*

Dr. Kin Wa Kwan, Prof. Alfonso H. W. Ngan
Department of Mechanical Engineering, the University of Hong Kong, Pokfulam Road, HKSAR. China
E-mail: kkwkwan@connect.hku.hk
Dr. Degang Xie, Ms. Rongrong Zhang, Prof. Zhiwei Shan
Center for Advancing Materials Performance from the Nanoscale (CAMP-Nano) & Hysitron Applied Research Center in China (HARCC), State Key Laboratory for Mechanical Behavior of Materials, Xi'an Jiaotong University, Xi'an 710049, China

Keywords: Nickel hydroxide-oxyhydroxide, turbostratic structures, phase transformation; *In situ* transmission electron microscopy (TEM)

Abstract: Water removal, phase transformation and crystallization of turbostratic nickel hydroxide and oxyhydroxide ($Ni(OH)_2$-NiOOH) are found to be inducible by the electron beam of a transmission electron microscope (TEM). Under 30 seconds of beam exposure at an accelerating voltage of 200 keV and a beam current density of 500 mA/m^2, the original, characteristic turbostratic structure of $Ni(OH)_2$-NiOOH is observed to disappear, caused by the quick removal of intercalated water molecules by the electron beam. Increasing the current density from a low value of 1.5 mA/m^2 to a high value of 500 mA/m^2 can transform the $Ni(OH)_2$-NiOOH into nickel oxide (NiO) in 1 minute. *In situ* heating and preheating experiments suggest that the transformation is caused by a heating effect induced by the electron beam. The results confirm that the mechanism previously discovered light-induced actuation of $Ni(OH)_2$-NiOOH is caused by desorption of water molecules.

1. Introduction

Nickel hydroxide and oxyhydroxide ($Ni(OH)_2$-NiOOH) material system is well known for its application as electrodes in rechargeable nickel cadmium and nickel hydride batteries. In addition, other potential applications have been demonstrated, including photocatalysis, electrocatalysis and electrosynthesis, supercapacitance, electrochromic devices and electrochemical sensors, as reviewed by Hall, et al..[1] Recently, actuation properties of anodic-electrodeposited $Ni(OH)_2$-NiOOH triggered by electrochemical reactions,[2] light and other means have been discovered,[3] and the properties are shown to be related to the disordered micro-structure named as "turbostratic" structure. As the light-induced actuation was found to be caused by the volume decrease resulted from desorption of intercalated water molecules under illumination,[3] we hypothesized that the removal of the water molecules can also be induced by electron beam under the transmission electron microscope (TEM) and therefore a direct evidence on the actuation mechanism may be found.

Moreover, microstructural characterization for the turbostratic $Ni(OH)_2$-NiOOH is challenging, since it is non-crystalline and may contain different degree of structural disorder[4, 5] in addition to the turbostratic α-$Ni(OH)_2$ and γ-NiOOH that were proposed by Bode, et al. half a century ago.[6] TEM has been a useful tool to identify the structure and crystallinity of $Ni(OH)_2$.[7-9] It was reported that crystalline $Ni(OH)_2$ can be changed into NiO under electron-beam irradiation,[10-13] however, there has been no report on the transformation of turbostratic $Ni(OH)_2$-NiOOH. Given that *in situ* TEM has been used to uncover the detailed mechanism of reactions utilized in many areas,[14-16] we performed a comprehensive TEM study, including *in situ* heating, on the water removal, phase transformation and crystallization of turbostratic $Ni(OH)_2$-NiOOH under electron-beam irradiation.

2. Experimental Section

2.1. Materials

Nickel sulfate heptahydrate ($NiSO_4 \cdot 7H_2O$) in purum p.a. grade, sodium acetate (NaOAc) and sodium sulfate (Na_2SO_4) in puriss p.a. grade, and sodium hydroxide (NaOH) in reagent grade were purchased from Sigma-aldrich and used as received.

2.2. Fabrication of turbostratic Ni(OH)2-NiOOH

Turbostratic $Ni(OH)_2$ and NiOOH were fabricated by anodic electrodeposition on fluorine doped tin oxide (FTO) glass followed by electrochemical reduction and oxidation.[2, 17] A thin layer of NiOOH was electrodeposited on FTO glass slides measuring 1 × 2 cm^2 in a 3-electrode plating bath of 0.13 M $NiSO_4$, 0.1 M NaOAc and 0.13 M Na_2SO_4 for 40 min under vigorous stirring. A constant current density of 0.4 mA/cm^2 was applied against the saturated calomel electrode (SCE) with platinum mesh as the counter electrode. After this procedure, a uniform, black or dark brown layer of NiOOH was observed as the electrodeposition product. To obtain $Ni(OH)_2$, 0 V was applied to the NiOOH fabricated on FTO against SCE in 1 M NaOH for 30 min, until the colour turned pale. To prevent unwanted reduction of NiOOH by moisture, the freshly-fabricated NiOOH was first oxidized at 0.4 V in 1 M NaOH for 30 min and then stored under a sealed dry box.

2.3. TEM Irradiation

A small droplet of deionized water was first placed on the $Ni(OH)_2$ or NiOOH fabricated on FTO. The $Ni(OH)_2$ or NiOOH thin layer underneath was then scratched off the FTO into small flakes with a pair of sharp tweezers. For the electron-beam exposure experiment, a drop of water containing flakes of $Ni(OH)_2$ or NiOOH was transferred onto a carbon film supported on a copper grid (Pelco®), followed by drying in air for around 15 min. The grid was then loaded onto the specimen holder for TEM examination. For the *in situ* heating experiment, a double tilt heating holder was used.

High-resolution TEM (HRTEM) images were taken in a JEOL JEM-ARM200F Cs-corrected TEM at the electron-beam current density of 1.5 mA/m^2. Short-time electron-beam exposure experiments were carried out in an FEI Tecnai G2 20 S-TWIN Scanning Transmission Electron Microscope. The electron-beam current was switched between 1.5 mA/m^2 and 500 mA/m^2 to study the effect of current density on the phase transformation. Long electron-beam exposure and *in situ* heating experiments were performed in a Hitachi H-9500 300 kV TEM.

3. Results

Figure 1 shows an HRTEM image of a $Ni(OH)_2$ sample, which manifests itself as a disordered structure as shown in the low-magnification image and the corresponding fast Fourier transform (FFT) pattern in Figure 1a. Despite no clear diffraction rings can be seen in the FFT, wavy fringes with spacings in the range 6.4 – 7.9 Å were seen in a higher magnification as shown in Figure 1b. However, under the electron irradiation, dynamic evolution of the structure was noted, and such fringes had their spacings reduced quickly in 30 s to the range of 2.4 and 2.2 Å as shown in Figure 1b.

In another $Ni(OH)_2$ sample under similar irradiation conditions, nano-crystals were observed (Figure 1c). Here, spherical crystallites emerged in the amorphous matrix. The magnified image in Figure 1d shows that the crystal planes are well-stacked, and the interplanar spacings are similar to that in Figure 1c, namely, 2.4, 2.0 and 1.5 Å, which match well with the (1 1 1), (2 0 0) and (2 2 0) planes of NiO. The NiOOH samples showed similar features under HRTEM (not shown), with the interplanar spacings of the NiO nano-crystals measured as 2.4, 2.1 and 1.5 Å. However, the spacings of the initial wavy fringes were smaller at 4.3 ± 0.4 Å.

The selected area electron diffraction (SAED) patterns of NiOOH and $Ni(OH)_2$ under a low electron-beam current density of 1.5 mA/m^2 exhibited broad halos characteristic of a structure with low crystallinity (**Figure 2a**). The interplanar spacings calculated from of the mean radii of the diffraction halos/rings are summarized in **Table 1**. The measured values for both samples are in reasonable agreement with the literature values of γ-NiOOH and α-$Ni(OH)_2$ respectively.[1]

However, when the electron-beam current density was increased to a high value of 500 mA/m^2, the SAED patterns for both NiOOH and $Ni(OH)_2$ transformed under 1 min (Figure 2b, c). Also, the rings became much sharper under the stronger electron irradiation. The SAED patterns of the transformed samples are similar to the FFT pattern of the nanocrystalline sample in Figure 1c, which again match well with the (1 1 1), (2 0 0) and (2 2 0) planes of NiO. Longer exposure under the electron-beam (1.5 h) increased the sharpness of these three rings significantly, and the rings themselves became less continuous (**Figure 3a**). Also, at least 3 outer rings which match the NiO structure could be observed.

Similar transformation was also observed during *in situ* heating from room temperature to 400 °C (Figure 3b). The resulting SAED pattern resembles closely that of NiO, which can also be observed in preheated NiOOH (400 °C, 1 h in air furnace) as shown in Figure 3c. The interplanar spacings for the transformed samples are given in **Table 2**. The samples transformed under electron-beam match better with the theoretical structure of NiO than under heating. Lastly, TEM images corresponding to transformation by *in situ* heating (Figure 3a) and electron beam (Figure 3b) are respectively shown in **Figure 4a** and **4b**. The samples had crystallized and shrunk after the transformation. From these results, it is concluded that NiOOH and $Ni(OH)_2$ would transform into NiO under strong electron-beam and heating.

4. Discussion

The wavy fringes observed in the HRTEM images are similar to those found in graphite,[18] which suggests that the NiOOH and $Ni(OH)_2$ samples were truly turbostratic. Turbostratic structures of γ-NiOOH and α-$Ni(OH)_2$ are known to form if water molecules intercalate between the basal planes of the hexagonal crystals of β-NiOOH and β-$Ni(OH)_2$, so that the basal planes are randomly perturbed with an increased spacing.[4] The observed quick refinement of the wavy fringes of the $Ni(OH)_2$ sample and the appearance of crystallites should be caused by the removal of water molecules by the electron-beam. The corresponding SAED or FFT pattern do not clearly indicate the phase, but it is likely that the crystallized form was β-$Ni(OH)_2$ and/or NiO. Nevertheless, the removal of the intercalated water molecules under TEM supports the previously proposed mechanism of the light-induced actuation of turbostratic $Ni(OH)_2$-NiOOH, which is the desorption of intercalated water molecules under light illumination that causes a volume decrease.[3] It is noted that no crystallization was observed in light-induced actuation,[3] which is likely because the light used to induce the actuation did not have enough intensity to induce crystallization.

The present observation of NiO nano-crystals suggests that parts of the sample were transformed by the electron-beam. This is supported by the quick transformation of turbostratic NiOOH and $Ni(OH)_2$ into crystalline NiO under high electron-beam current density as indicated by the SAED patterns. Although the possibility for the transient formation of crystallized phases β-$Ni(OH)_2$ and β-NiOOH during the transformation cannot be excluded, the low crystallinity of the NiO as indicated by the SAED patterns favours the conclusion of direct transformation from turbostratic $Ni(OH)_2$-NiOOH into NiO.

Under a long exposure at a high electron-beam current density, even the higher-order outer rings became visible in the SAED pattern, implying a complete transformation from NiOOH or $Ni(OH)_2$ into NiO. The sharp and discontinuous innermost rings indicate significant crystallization and volume shrinkage as supported from the TEM images. The similar changes under *in situ* heating and preheating confirm that the transformation was

caused by the thermal effect induced by the electron beam. Note that the interplanar spacings of the NiO formed under heating do not match the theoretical values as well as those under electron-beam irradiation. This suggests that the electron-beam exposure can induce more complete transformation into NiO. Lastly, as the transformation into NiO occurs rapidly, erroneous characterization may be resulted. Verifying the TEM results when characterizing turbostratic $Ni(OH)_2$-NiOOH by varying the exposure time of electron-beam is necessary.

5. Conclusion

The microstructural change of electrodeposited turbostratic NiOOH and $Ni(OH)_2$ was studied by *in situ* TEM. The disappearance of fringes of the turbostratic structure under electron-beam was observed, which was caused by the removal of intercalated water. This observation confirms that light-induced actuation is caused by the volume decrease from water desorption. Besides, direct transformation of the turbostratic structure into crystalline NiO was found, which can quickly occur under an electron-beam current density of 500 mA/m^2. Similar transformation was also noted by *in situ* heating or pre-heating the samples, thus the electron-irradiation induced transformation is likely caused by thermal effects of the electron beam. These results show that NiOOH and $Ni(OH)_2$ are unstable under intense or prolonged electron-beam exposure, and so extra attention should be paid in the characterization of turbostratic $Ni(OH)_2$- NiOOH under TEM.

Acknowledgements

The work was funded by a grant from the Kingboard Endowed Professorship in Materials Engineering. The HRTEM characterization of this research work was carried out on the Cs-corrected TEM JEOL ARM200CF (project no. C6021-14E) at the Materials Characterization and Preparation Facility, the Hong Kong University of Science and Technology.

Received: ((will be filled in by the editorial staff))
Revised: ((will be filled in by the editorial staff))
Published online: ((will be filled in by the editorial staff))

References

[1] D.S. Hall, D.J. Lockwood, C. Bock, B.R. MacDougall, *Proc. R. Soc. A* **2015**, 20140792.

[2] K.W. Kwan, N.Y. Hau, S.P. Feng, A.H.W. Ngan, *Sens. Actuators. B Chem.* **2017**, *248*, 657.

[3] K.W. Kwan, S.J. Li, N.Y. Hau, W.-D. Li, S.P. Feng, A.H.W. Ngan, *Science Robotics* **2018**, *3*, eaat4051.

[4] P. Oliva, J. Leonardi, J. Laurent, C. Delmas, J. Braconnier, M. Figlarz, F. Fievet, A. De Guibert, *J. Power Sources* **1982**, *8*, 229.

[5] C. Faure, C. Delmas, M. Fouassier, *J. Power Sources* **1991**, *35*, 279.

[6] H. Bode, K. Dehmelt, J. Witte, *Electrochim Acta* **1966**, *11*, 1079.

[7] Y. Luo, G. Li, G. Duan, L. Zhang, *Nanotechnology* **2006**, *17*, 4278.

[8] C. Liu, Y. Li, *J. Alloys Compd.* **2009**, *478*, 415.

[9] M. Casas-Cabanas, J. Canales-Vázquez, J. Rodríguez-Carvajal, M.R. Palacín, *J. Am. Chem. Soc.* **2007**, *129*, 5840.

[10] J. Li, W. Zhao, F. Huang, A. Manivannan, N. Wu, *Nanoscale*, **2011**, 3, 5103.

[11] L. Dong, Y. Chu, W. Sun, *Chem-Eur J.* **2008**, *14*, 5064.

[12] K. Matsui, T. Kyotani, A. Tomita, *Adv. Mater.* **2002**, *14*, 1216.

[13] S. Sarkar, M. Pradhan, A.K. Sinha, M. Basu, Y. Negishi, T. Pal, *Inorg. Chem.* **2010**, *49*, 8813.

[14] Y. Yang, X. Liu, Z. Dai, F. Yuan, Y. Bando, D. Golberg, X. Wang, *Adv. Mater.* **2017**, *29*, 1606922.

[15] X.H. Liu, Y. Liu, A. Kushima, S. Zhang, T. Zhu, J. Li, J.Y. Huang, *Adv. Energy. Mater.* **2012**, *2*, 722.

[16] X. Wang, Q. Weng, Y. Yang, Y. Bando, D. Golberg, *Chem. Soc. Rev.*, **2016**, *45*, 4042.

[17] Y.-H. Chang, N.Y. Hau, C. Liu, Y.-T. Huang, C.-C. Li, K. Shih, S.-P. Feng, *Nanoscale*, **2014**, *6*, 15309.

[18] D. Singh, *J. Electrochem. Soc.* **1998**, *145*, 116.

[19] S. Dimovski, A. Nikitin, H. Ye, Y. Gogotsi, *J. Mater. Chem.* **2004**, *14*, 238.

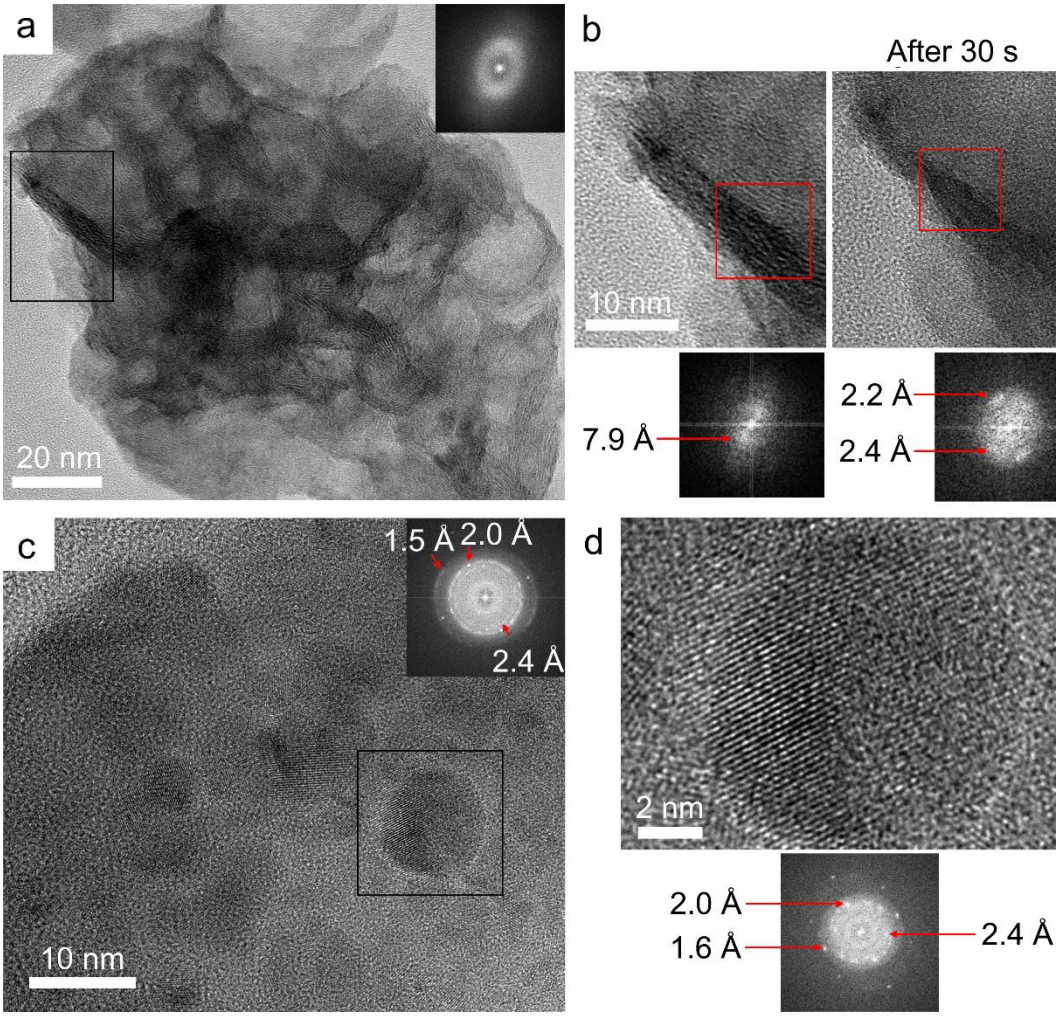

Figure 1. High-resolution TEM images and FFT of (a) a turbostratic part of $Ni(OH)_2$; (b) magnified images of a region in (a) showing the refinement of wavy fringes during 30 s of electron irradiation. (c) Another $Ni(OH)_2$ specimen undergoing similar irradiation, with nano crystallites of NiO emerged; (d) shows magnified image of a nano-crystal in (c).

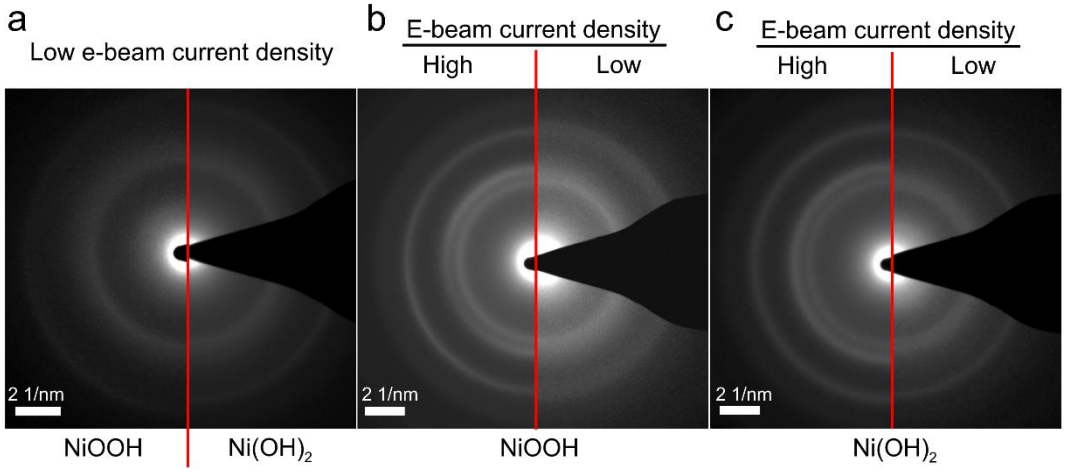

Figure 2. SAED patterns of $Ni(OH)_2$-NiOOH under the conditions: (a) NiOOH and $Ni(OH)_2$) under low electron-beam current density; (b,c) NiOOH and $Ni(OH)_2$ samples under high and low electron-beam current density with a short exposure time.

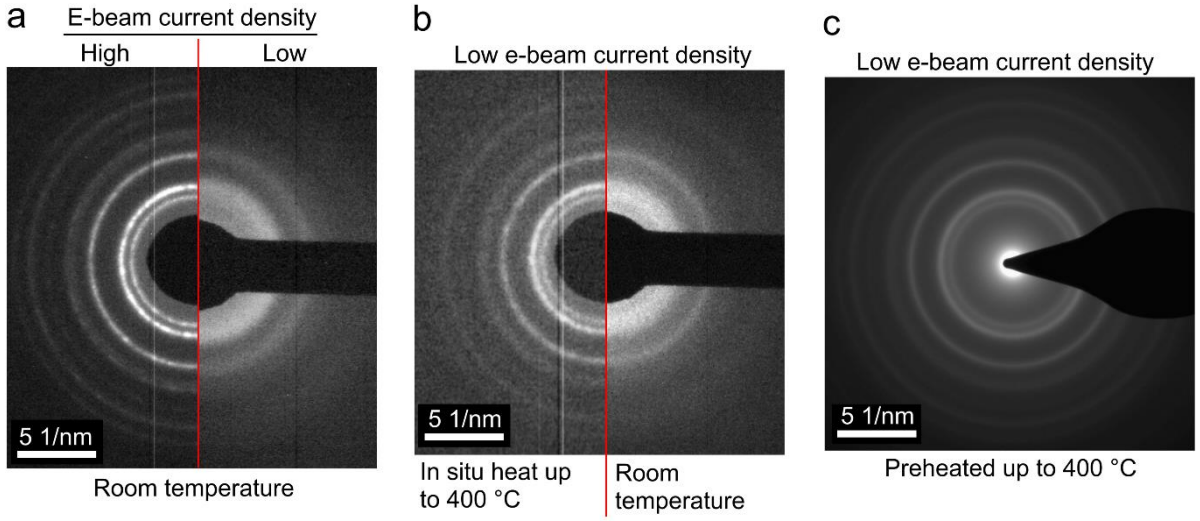

Figure 3. SAED patterns of NiOOH under the conditions: (a) Long exposure at high and low electron-beam current density; (b) *in situ* heating up to 400 °C and at room temperature; (c) preheating to 400 °C and observed under low electron-beam current density.

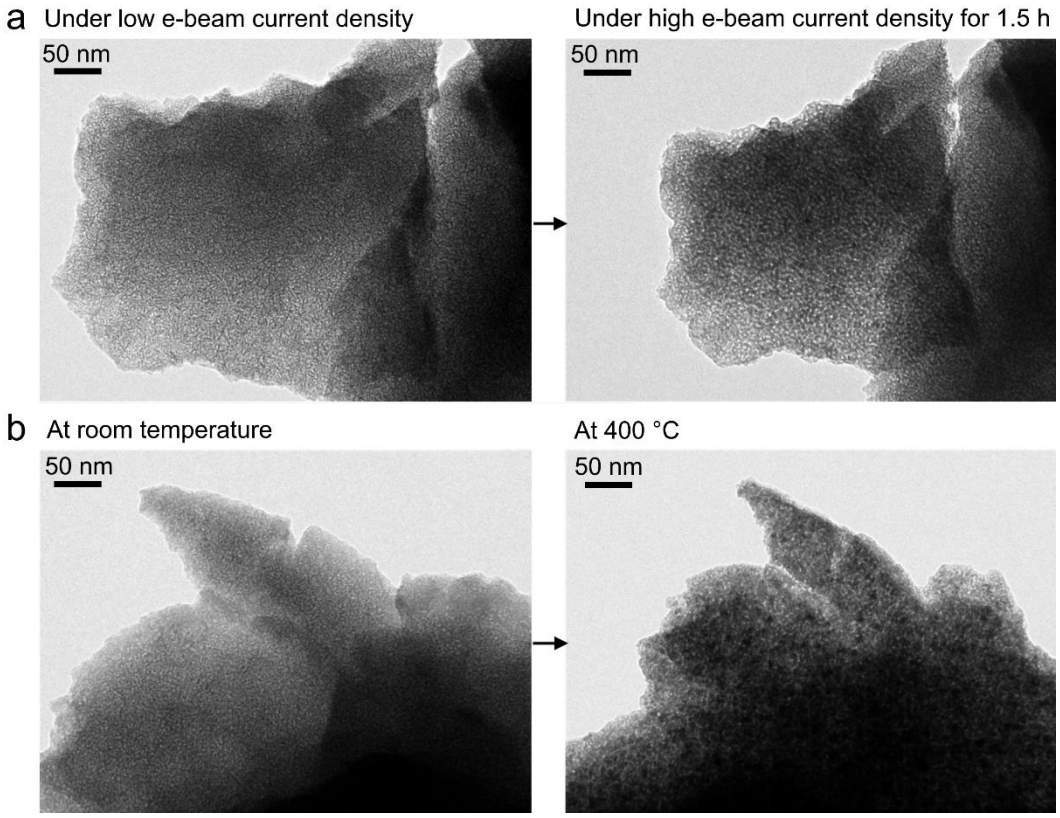

Figure 4. TEM images showing the transformation of the samples (a) under high electron-beam current density corresponding to Figure 3a and (b) in-situ heating 400 °C corresponding to Figure 3b.

Table 1. The interplanar spacings calculated from the SAED patterns of NiOOH and $Ni(OH)_2$ under low electron-beam current density and the literature values.

	γ-NiOOH Sample	Literature values [19]	α-$Ni(OH)_2$ Sample	Literature values [1]
Interplanar spacing (Å)	2.41 ± 0.03	(1 0 1): 2.42	2.57 ± 0.02	(1 1 0): 2.67
	1.42 ± 0.01	(1 1 0): 1.41	1.56 ± 0.00	(3 0 1): 1.50

Table 2 The calculated interplanar spacings for NiOOH and $Ni(OH)_2$ under high electron-beam current density, that of in-situ heating and preheating under low electron-beam current density, and the theoretical values of NiO.

	Sample				
	NiOOH	$Ni(OH)_2$	In-situ 400 °C	Preheated 400 °C	**Theoretical values of NiO**
Electron-beam current density	High		Low		
Interplanar spacing (Å)	2.49	2.44	2.56	2.54	(1 1 1): 2.41
	2.16	2.12	2.19	2.21	(2 0 0): 2.09
	1.50	1.49	1.56	1.56	(2 2 0): 1.47
	/	/	1.30	1.29	(3 1 1): 1.26
	1.23	1.22	/	/	(2 2 2): 1.20
	/	/	/	1.10	(4 0 0): 1.04
	0.95	0.94	0.99	0.99	(3 3 1): 0.96
	/	/	/	0.91	(4 2 0): 0.93